

Novel Synthetic Aperture Radar Imaging Techniques

Patricia Wright
BAE SYSTEMS Advanced Technology Centre
West Hanningfield Road
Great Baddow
Chelmsford, CM2 8HN

Abstract

Currently, a number of new synthetic aperture radar (SAR) imaging techniques are under development by various non-UK groups world wide. There is a real danger that the UK will be left behind as these technology areas are developed. The aim of this work is to review the current status and to encourage the use of these techniques within the UK. The focus of this paper is on two of the new SAR technology: along track interferometry (ATI) and SAR tomography. To date these have been primarily demonstrated for civilian applications such as ocean monitoring and vegetation profiling. In this paper, we review these techniques and consider their suitability as defence technologies.

Keywords: SAR tomography, along-track interferometry, GMTI

Introduction

Along-track interferometric (ATI) synthetic aperture radar (SAR) is a remote sensing technique, which offers a means of monitoring moving targets. The basis of the technique is that the interferometric combination of two complex SAR images of the same scene, acquired with a short time lag, is sensitive to the Doppler shift from the line-of-sight velocity of targets. The use of ATI for Ground Moving Target Imaging (GMTI) from space and air is now being considered by many groups worldwide [1,2,3]. Tomography is a technique which determines the 3D structure of a volume from measurements made outside the volume and facilitates localisation of scatterers within the volume. Recently, interest has grown in applying tomographic techniques to SAR imaging. This can be achieved by the formation of an additional aperture in elevation, through a coherent combination of images acquired from several parallel imaging points with different elevations. Tomographic SAR is currently being explored by DARPA as a potentially complementary technique to

FOPEN to provide under-foliage target detection.

ATI SAR

In ATI, at least two antennas, displaced in azimuth by L , are deployed on a platform moving at speed V . Figure 1 shows a basic ATI geometry, where only one antenna receives. The receive channels do not need to be formed by separate antennas, but may be a single antenna configured to receive on two independent phase centres.

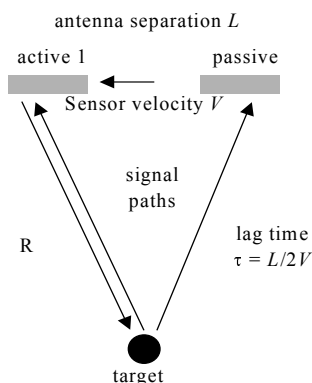


Figure 1. ATI imaging geometry at a fixed time

If the target has a velocity component in range, in the image it is also shifted in azimuth by:

$$\Delta az = \frac{V_{rad}}{V} R \quad (1)$$

where V_{rad} is the target range rate and R is the slant range distance to the target. If an interferogram I is formed from the active image at location 1 and the passive image, at location 1 at a time τ later, then the target range velocity gives an interferometric phase shift. I is formed using (2), where S_1 and S_2 are the complex SAR images, ϕ_1 and ϕ_2 are the phases of the complex data and the subscripts 1 and 2 denote the images from the fore and aft antennas.

$$I = S_1 S_2^* = |S_1| |S_2| \exp[j(\phi_1 - \phi_2)] \quad (2)$$

After registration of the aft channel to take account of the time shift $L/2V$, the interferometric phase difference between the two received signals is:

$$\Delta\phi = \phi_2 - \phi_1 = -\frac{kL^2}{4R} + \frac{kL}{V} V_{rad} \quad (3)$$

where k is the radar wavenumber. The first term in (3) is a range-dependent phase, which may produce a significant phase gradient across a swath for systems with large antenna separations. The second term depends on the slant-range component of the target's velocity and this is the term of interest to retrieve information about target motion. Equation (3) indicates that the accuracy of the target range rate measurements depends on the antenna separation, the sensor wavelength, and the aircraft speed. Because the target has to be detected against a noisy background, other factors include the signal to noise ratio, the signal to clutter ratio and the interferometric coherence [1].

Design of an ATI sensor is determined by (3) and the velocity range of the moving targets to be measured. The sensor must be designed with a lag time suited to the target velocity.

For slow moving targets, phase noise limits the minimum detectable velocity. If the phase noise is large, the signal of a small target velocity will be lost in the noise. The phase noise is related to the signal to noise ratio (SNR) through the interferometric coherence, as follows:

$$\gamma = \frac{\gamma_t}{1 + SNR^{-1}} \quad (4)$$

where γ_t is the temporal decorrelation for scatterers within the scene. This coherence determines the phase noise of the data:

$$\sigma_\phi = \frac{1}{\sqrt{2N}} \frac{\sqrt{1-\gamma^2}}{\gamma} \quad (5)$$

Table 1 gives theoretical retrieval accuracies for an X-band sensor travelling at 200 m/s with a 1m antenna separation, for a variety of scene coherence values. Coherence of 0.99 is near perfect and will generally occur for thinly vegetated regions, or longer wavelengths.

Phase Noise (radians)	Scene coherence	V_{rad} accuracy	
		m/s	km/h
1.225	0.50	1.17	4.20
0.412	0.75	0.40	1.44
0.101	0.99	0.09	0.35

Table 1 Coherence impact on velocity retrieval

The stationary elements of the two scenes should have zero differential phase. However, in actual data, stationary elements will contain contributions from the radar phase noise. Also, moving targets can have non-zero clutter contribution (depending on the target and resolution cell sizes). For these cases, accurate detection and velocity estimation can be challenging, requiring the use of probabilistic detection algorithms [2]. Detection probability of moving targets can be increased by the use of space-time adaptive filtering (STAP). Here, statistical modelling of the ATI phase signal of targets plus clutter and noise allows an optimal detector to be designed [3].

Canada's Department of National Defence (DND) are running a C-band (5.3GHz), HH polarisation airborne GMTI demonstration project [3]. In the experiment, corner reflectors, mounted on a variety of transport systems, were used to simulate vehicle targets (MVT, smaller infantry targets (MIT), and pick-up trucks (PU). The background terrain radar cross section (RCS) was low for the controlled targets, resulting in high target-to-clutter ratios. Table 2 summarises the target velocities and RCS.

Initial candidate targets were detected by zeroing the amplitude of scatterers with phase signals lying within a threshold keyhole filter [4], determined by analysing the phase distribution of the clutter. A

Target	Speed (km/h)	RCS(m ²)
MVT-1	20, 30	706
MVT-2	10,20	309
MIT-1	5	24
PU-1	50,70	434
PU-2	40,60	432

Table 2 Targets in a GMTI demonstration.

suitable moving target matched filter (MTMF) is then applied, allowing velocity adapted SAR processing of each target, reducing the clutter contribution. Maximum target power results from an MTMF produced using a velocity similar to the target velocity [3]. This data is then ATI processed to provide velocity estimates.

The only target not consistently detected in the experiment was the slow moving MIT target. The rms error in velocity measurement was 3.34km/h for the ATI technique (compared with 3.66km/h for Displaced Phase Centre Array techniques applied to the same data). Overall, the ATI technique resulted in velocity estimates accurate to within 5%.

SAR Tomography

In SAR tomography, 3D image reconstruction is achieved by inverting a set of 2D images which represent different projections of the object [5].

The resolution which can be achieved in elevation by such a SAR system is given by

$$\rho_n = \frac{s\lambda}{2L_n} \quad (6)$$

where s is the mean slant range to the point on the ground for all the flight paths, λ is the wavelength of the radar sensor and L_n is the length of the aperture synthesised in elevation. Improved elevation resolution can be achieved by use of a short wavelength or synthesis of a longer elevation aperture. However, in general, longer wavelengths, such as L- and P-band (1.25GHz and 400MHz respectively) are preferred for SAR tomography, as they ensure high penetration into a volume. This can for example, facilitate imaging of scatterers under foliage. Resolution improvement, therefore, is mainly to be achieved by synthesising an appropriate elevation aperture length.

The radar signal r scattered from an object may be represented as:

$$r(z, n_0) = o(s_0, n_0) * \exp\left(-\frac{ik}{s_0}(z - n_0)^2\right) \quad (7)$$

where the object is at height n_0 , and slant range s_0 the sensor at height z . The first step in tomographic processing involves deramping the SAR signal to remove the quadratic phase variation in (7) followed by a phase correction to a constant slant range distance. This latter correction is required as, in the real world, the flight tracks will be separated in slant range as well as in elevation. The deramped signal is:

$$r_i(z, n_0) = o(s_0, n_0) * \exp\left(-\frac{ik}{\langle s \rangle}(n_0^2 - 2B_{ni}n_0)\right) \quad (8)$$

where B_{ni} is the separation between flight tracks i and $i+1$, perpendicular to the slant range direction. The tomographic image is

then formed by applying a Fourier transform in elevation to the N images, thereby focussing the tomographic image in elevation.

$$R_i(k_z, n_0) = 1/N \sum_{i=1}^N r_i \exp\left(\frac{2ik}{\langle s \rangle} n B_{ni}\right) \quad (9)$$

Given the sparse nature of the elevation aperture, elevation ambiguities can be strong. These can be suppressed by synthesising data at additional flight path locations and resampling the tomographic data to an even flight path spacing. Data synthesis is achieved by forming interferograms (I) between images i and $i+1$:

$$I_{i,i+1} = o(s_0, n_0)^2 \exp\left(-\frac{ik}{\langle s \rangle} (2\Delta B_{n;i,i+1} n_0)\right) \quad (10)$$

Using interferogram I , for every sensor separation B_n , two new tracks can be simulated at positions $B_{nj} \pm \Delta B_{n;i,i+1}$, i.e.:

$$S_j^+ = S_j * I / |I| = o(s_0, n_0) \exp\left(-\frac{ik}{\langle s \rangle} (n_0^2 - 2(B_{n;j} + \Delta B_{n;i,i+1}) n_0)\right) \quad (11)$$

With the addition of synthesised flight paths, the data can be resampled to an even spacing. The results are shown in Figure 2 [5].

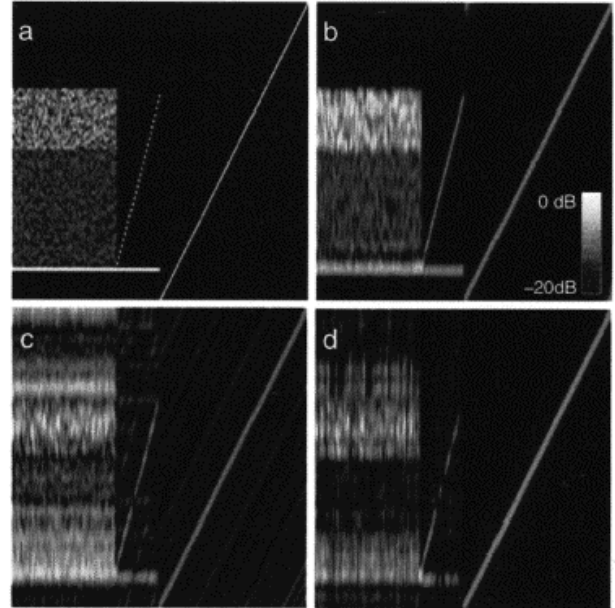


Figure 2 Ambiguity suppression in tomographic data

Element a of the figure shows simulated scatterers. On the left is a three layer volume with two layers of distributed random scatterers over a surface. The horizontal direction is azimuth and the vertical is elevation. In the middle of the image there are two discrete scatterers with different height separations and on the right of the image a single scatterer placed at different heights. Element b shows the resulting tomographic image with ambiguity suppression and resampling of the data. Element c) shows the tomographic image from irregularly spaced flight paths, with no ambiguity suppression. Element d) shows the tomographic image with ambiguity suppression but without interpolating the data to be evenly sampled. In the case of the single scatterer at various height positions, ambiguity suppression without resampling is sufficient to provide a clean tomographic image of the scatterer. Although, for the two and three layer simulation data ambiguity suppression improves the data quality, only with elevation resampling is clean tomographic imagery achieved. In particular, in element b), the tomographic processing with ambiguity suppression and

resampling is able to discern the scattering surface under two layers of randomly distributed volume scatterers.

An actual tomographic SAR image [5] is shown in Figure 3. Scattering signatures of different objects (the ground, buildings, cars, trees and a corner reflector) and their elevations at different polarisations are clearly illustrated in a) to c).

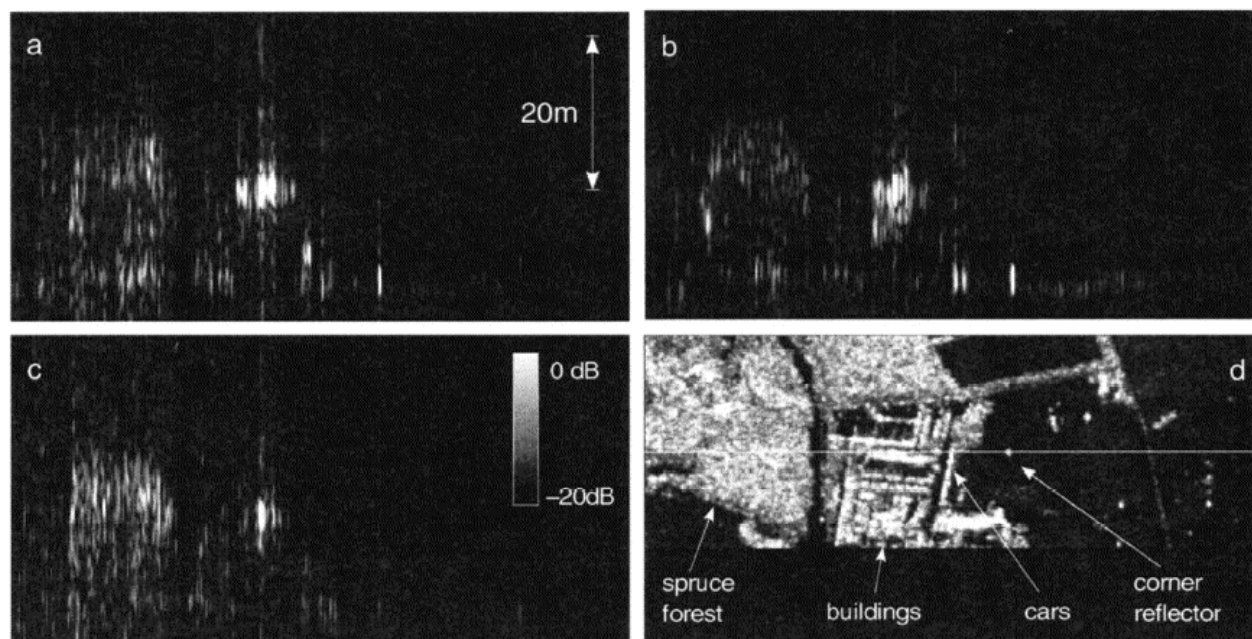


Figure 3 A single azimuth slice of tomographic data a) HH polarisation, b)VV polarisation, c) HV polarisation, d) amplitude image showing the azimuth line illustrated [5]

Closer inspection of the VV polarisation image shows a strong return at ground level for the cars and a much weaker elevated return for the forest canopy (tree height 15-20m). The images suggest the potential for under-foliage target detection using this technique.

Summary

In order to gain a better understanding of new SAR imaging techniques and determine how they can be used to extend UK defense and civilian RF capabilities we have performed a review of two novel SAR techniques. Firstly we reviewed ATI for GMTI, also considering the use of azimuth

squinting to improve information content and compared ATI with DCPA results. We identified factors affecting sensitivity to target velocity including wavelength, polarisation, separation of radar elements, and clutter strength.

The second novel SAR topic considered was that of tomographic SAR. We have reviewed the theory behind tomographic SAR and shown simulated and real results available from the literature indicating its capability. We have reviewed a number of factors affecting foliage penetration including wavelength, polarisation, choice of baselines and the need for ambiguity suppression.

References

- [1] Pascazio, V., Schirinzi, G., Farina, A., 2001, "Moving Target Detection by Along Track Interferometry", Proceedings of IGARSS, 2001.
- [2] Beaulne, P. et al, 2003, "Preliminary design of a SAR-GMTI processing system for Radarsat-2 Modex data", IGARSS 03.
- [3] Livingstone, C.E et al., "An airborne synthetic aperture radar (SAR) experiment to support RADARSAT-2 ground moving target indication (GMTI)", Can. Journal Remote Sensing, Vol. 28, No.6, 2002
- [4] Chiu, S., et al., 2000, "Computer simulations of Canada's Radarsat-2 GMTI", Proceedings RTO SET Symposium on "Space-based Observation Technology", 2000.
- [5] Reigber, A. and Alberto Moreira, 2000, "First Demonstration of Airborne SAR Tomography Using Multibaseline L-Band Data", IEEE TGARS, Vol. 38, No. 5.